

AD-A262 997



DOCUMENTATION PAGE

Form Approved
OMB No. 0704-0188

ation is estimated to average 1 hour per response, including the time for reviewing instructions, searching existing data sources, gathering and reviewing the collection of information, sending comments regarding this burden estimate or any other aspect of this reducing this burden. Send comments to Washington Headquarters Services, Directorate for Information Operations and Policy, 1215 Jefferson Ave., and to the Office of Management and Budget, Paperwork Reduction Project (0704-0188) in Washington, DC 20503.

2. REPORT DATE

19 March 1993

3. REPORT TYPE AND DATES COVERED

Technical

4. TITLE AND SUBTITLE

The Mechanical Response of Gold Substrates Modified with Self-Assembling Monolayer Films.

5. FUNDING NUMBERS

N00014-91-1991

6. AUTHOR(S)

Ross C. Thomas and Richard M. Crooks*
J. E. Houston and Terry A. Michalske*

7. PERFORMING ORGANIZATION NAME(S) AND ADDRESS(ES)

*Department of Chemistry
University of New Mexico
Albuquerque, NM 87131*Surface Science Dept. 1114
Sandia National Laboratories
Albuquerque, NM 871858. PERFORMING ORGANIZATION
REPORT NUMBER

4

9. SPONSORING / MONITORING AGENCY NAME(S) AND ADDRESS(ES)

Office of Naval Research
800 North Quincy Street
Arlington, VA 22217-500010. SPONSORING / MONITORING
AGENCY REPORT NUMBER

APR 20 1993

11. SUPPLEMENTARY NOTES

Prepared for Publication in *Langmuir*

12a. DISTRIBUTION / AVAILABILITY STATEMENT

This document has been approved for public release and sale;
its distribution is unlimited

12b. DISTRIBUTION CODE

N00179

13. ABSTRACT (Maximum 200 words)

We have used the newly developed interfacial force microscope (IFM) to study the adhesive and mechanical properties of a Au substrate. We show that a W probe interacting with a Au surface results in plastic deformation under very small repulsive loads and transfers Au to the probe surface in a galling interaction upon removal. However, when the Au surface is passivated by a self-assembling monolayer of *n*-docosane thiol molecules (CH₃(CH₂)₂₁SH), the substrate is able to elastically support large repulsive loads with no attractive interactions. Within this elastic region, the load/deformation relationship closely follows the classic Hertzian model for a rigid punch deforming an elastic half space. As a result, we are able to determine the maximum values for the shear-stress threshold for plastic deformation to be approximately 1 GPa in agreement with theoretical determinations. Above this value, the substrate permanently deforms. Remarkably, however, the strong binding of the molecular film to the Au surface permits it to maintain its passivating properties even after gross plastic damage.

14. SUBJECT TERMS

15. NUMBER OF PAGES

16. PRICE CODE

17. SECURITY CLASSIFICATION
OF REPORT

Unclassified

18. SECURITY CLASSIFICATION
OF THIS PAGE

Unclassified

19. SECURITY CLASSIFICATION
OF ABSTRACT

Unclassified

20. LIMITATION OF ABSTRACT

DTIC QUALITY ASSURANCE 4

OFFICE OF NAVAL RESEARCH

GRANT N00014-91 J-1991

R&T Code s400x084yi01

Technical Report No. 4

Accession For	
NTIS CRA&I	<input checked="" type="checkbox"/>
DTIC TAB	<input type="checkbox"/>
Unannounced	<input type="checkbox"/>
Justification	
By	
Distribution/	
Availability Codes	
Dist	Avail and/or Special
A-1	

The Mechanical Response of Gold Substrates Modified with Self-Assembling Monolayer Films

by

Ross C. Thomas and Richard M. Crooks

Department of Chemistry

University of New Mexico

Albuquerque, NM 87131

and

J. E. Houston and Terry A. Michalske

Surface Science Department 1114

Sandia National Laboratories

Albuquerque, NM 87185

Prepared for Publication

in

Science

March 19, 1993

Reproduction in whole or in part is permitted for any purpose of the United States Government.

This document has been approved for public release and sale;
its distribution is unlimited.

The Mechanical Response of Gold Substrates Modified with Self-Assembling Monolayer Films

Ross C. Thomas, J. E. Houston, Terry A. Michalske, and Richard M. Crooks

Abstract

We have used the newly developed interfacial force microscope (IFM) to study the adhesive and mechanical properties of a Au substrate. We show that a W probe interacting with a Au surface results in plastic deformation under very small repulsive loads and transfers Au to the probe surface in a galling interaction upon removal. However when the Au surface is passivated by a self-assembling monolayer of *n*-docosanethiol molecules ($\text{CH}_3(\text{CH}_2)_{21}\text{SH}$), the substrate is able to elastically support large repulsive loads with no attractive interactions. Within this elastic region, the load/deformation relationship closely follows the classic Hertzian model for a rigid punch deforming an elastic half space. As a result, we are able to determine the maximum values for the shear-stress threshold for plastic deformation to be approximately 1 GPa in agreement with theoretical determinations. Above this value, the substrate permanently deforms. Remarkably, however, the strong binding of the molecular film to the Au surface permits it to maintain its passivating properties even after gross plastic damage.

Ross C. Thomas and Richard M. Crooks are in the Department of Chemistry, University of New Mexico, Albuquerque, New Mexico 87131. J. E. Houston and Terry A. Michalske are in the Surface Science Department, Division 1114, at Sandia National Laboratories, Albuquerque, New Mexico 87185

Introduction

Several recent studies have demonstrated the ability of monolayer-level films of organic molecules to passivate the strong adhesive interaction between metal surfaces (1-5). For example, we have used the newly developed interfacial force microscope (IFM) (6) to study the behavior of a methyl terminated n-hexadecanethiol ($\text{CH}_3(\text{CH}_2)_{15}\text{SH}$) monolayer film adsorbed on a Au surface (1). We found a negligible adhesive interaction between a W probe and either the methyl-terminated film surface or the underlying Au substrate surface even at loads capable of permanent Au deformation (1, 2). These studies strongly suggest that such films could become important as surface-specific lubricants with very high breakdown resistance.

In the present paper, we expand our earlier studies to quantitatively evaluate how a thin organized monolayer film changes the mechanical interaction between a Au surface and a W probe. Specifically, we show that below substrate shear stress levels of approximately 1.0 GPa, the deformations are consistent with those expected from a Hertzian model involving a rigid, non-interacting punch elastically deforming a substrate. This behavior is in stark contrast to the situation observed in the absence of the monolayer film where we find, in agreement with recent experimental and theoretical results (4, 5), that permanent damage occurs under negligible loads and there is a transfer of Au to the probe surface. For higher stress levels, in the presence of the film, the surface is found to permanently deform. However, the passivating properties of the film are maintained even after considerable plastic deformation. Thus, not only are these findings supportive of the unique lubricating behavior of the thiol monolayers on Au, but they also indicate that such films can play an important role in facilitating studies of the nano-scale mechanical properties of materials.

Experimental Aspects

Self-assembling monolayer films confined to Au surfaces are particularly good model systems for adhesion and lubrication studies since the film structures are well understood as a result of extensive analyses by optical ellipsometry, electrochemistry, transmission electron microscopy, low energy electron diffraction, neutron diffraction, x-ray diffraction and x-ray photoelectron spectroscopy (7-10). These studies indicate that the sulfur head groups of *n*-alkanethiols strongly bind to a specific site on the Au (111) surface to form a Au(I)-thiolate species. The aliphatic portion of the molecules interact through intermolecular van der Waal's forces causing the surface-confined structures to form well-ordered and densely packed assemblies with their molecular axes tilted 25-30° from the surface normal.

In the present studies, the monolayer films were prepared by soaking Au substrates in 0.5 mM *n*-docosanethiol solutions in purified hexadecane for 24 h. Substrates were prepared by e-beam vapor deposition of 20 nm of Ti followed by 200 nm of Au onto Si (100) surfaces. Immediately before adsorbing the organic films, the Au substrates were cleaned in a 3:1 concentrated H₂SO₄:30% H₂O₂ solution. Freshly prepared monolayer surfaces were thoroughly rinsed with hexadecane and dried with N₂. The films were characterized by ellipsometry and Fourier transform infrared external reflectance spectroscopy prior to IFM studies. The thickness and vibrational spectra agreed with those reported previously (9,11).

We recently introduced the interfacial force microscope (IFM) specifically to study interfacial interactions between carefully characterized and controlled surfaces and image this interaction with nanometer resolution in both the attractive and repulsive scanning modes. The IFM compliments and expands the capabilities of existing interfacial force instruments such as the surface forces apparatus (12), the nanoindenter (13), and the atomic force microscope (5). The IFM's expanded capability stems from its differential-capacitance force sensor that uses a self-balancing force-feedback scheme. This feature permits quantitative interfacial-force

measurements and eliminates the mechanical instability encountered in deflection-based force sensors--the so-called "jump-to-contact" effect (5, 14).

The present IFM measurements were carried out in a low pressure chamber evacuated to 10^{-8} mmHg and then backfilled with 1 atm of dry N_2 . The W probe was characterized by scanning electron microscopy (SEM) and found to have a parabolic shape with a radius of curvature at the apex of approximately 500 nm. At the start of each experiment, contaminants were field desorbed from the W probe by applying 300 V to the tip in series with a 52 M Ω resistor. This procedure desorbs all but the most tightly bound species leaving only small amounts of chemisorbed C and O (15). IFM loading data were obtained in the force-feedback mode by bringing the sample from probe-sample separations of a few nanometers into repulsive contact up to a specified load level and then returning to the original position at a constant rate of 5 nm/sec. Force images were taken in the repulsive mode at a constant load level of 0.2 μ N.

Results and Discussion

A typical loading cycle for an *n*-docosanethiol film is shown in Fig. 1A up to repulsive loads of almost 15 μ N, where positive displacements indicate repulsive forces. The zero separation value is arbitrarily chosen to represent the starting point of the sample approach. Several features are evident from these results: 1) no appreciable attractive behavior is detected at any point in the cycle, 2) the interfacial force becomes repulsive at a displacement value of approximately 2 nm, increases and reaches a maximum load of just less than 15 μ N at about 5.6 nm and 3) upon reversal, the loading curve is retraced down to a load level near 3 μ N at which point a hysteresis "loop" opens with the interfacial force falling more rapidly than it rose upon approach. These results are in keeping with our earlier findings for a *n*-hexadecanethiol film on Au (1, 2): 1) the inert methyl-terminated surface of the film

produces a negligible adhesive interaction with the W probe, 2) the hysteresis loop results from the time-dependent response of the film being compressed between the probe and substrate surface, 3) when the loop closes at higher loads, the film is fully compressed and the observed deformation represents the elastic response of the substrate surface and 4) even at the highest loads, which elastically deform the Au, no adhesive probe/substrate interaction is observed.

If the monolayer film eliminates the adhesive interaction between the probe and substrate surface, then the loading behavior of Fig. 1A can be analyzed by simple Hertzian (16) contact mechanics to obtain a more quantitative measure of the stresses and deformations produced during the experiments. Modeling the system as a noninteracting, rigid parabolic punch deforming an elastic half space indicates that after contact the applied load will scale as the three halves power of the surface displacement (16). The unloading portion of Fig. 1A is shown in Fig. 1B, along with a Hertzian model curve (the solid line). We have only analyzed the unloading portion of the cycle of Fig. 1A since it is least affected by the mechanical properties of the film (1). The model curve was obtained by performing a least-squares fit to a three-halves power, offset-displacement function over the region from 4 to 5.6 nm to determine both the prefactor for the Hertzian equation (16) and the offset origin. This allows us to plot the resulting model function down to the contact point by analytic continuation. The fact that the Hertzian model function provides an excellent fit over a large portion of the unloading curve in Fig. 1B lends credibility to the purely elastic contact-mechanics model and permits a determination of the probe-tip dimensions and the contact stresses in the substrate. The resultant tip radius is 375 nm (the probe has a parabolic shape and this value represents the radius of curvature at the apex). Following this approach (16), we find that for a load of 15 μN the monolayer-modified Au substrate is exposed to a maximum compressive stress of 3.4 GPa. Subsequent

elastic analysis indicates that this loading condition results in a maximum substrate shear stress of 1.0 GPa (17) .

From a materials standpoint, it is remarkable that the maximum stress level applied during elastic contact is comparable to the calculated theoretical shear strength for Au (18). It is likewise remarkable that the self-assembling film resists being displaced and continues to passivate or lubricate the Au surface under such high-stress values.

To underscore the unique behavior just described, we show in Fig. 2A the contrasting results for a W probe interacting with a Au surface in the absence of the thiol film. The substrate was prepared by cleaning in a concentrated H_2SO_4 :30% H_2O_2 solution immediately prior to imaging. For this surface, we observe a slight repulsive wall at a relative displacement of approximately 48 nm that we attribute to the probe making contact with a non interacting layer of surface contamination, probably consisting of adventitious hydrocarbons and water (5). At a repulsive load near 0.4 μN , the probe begins to force the contaminant layer out of the way and starts to develop an adhesive bond to the Au substrate at a displacement of about 27 nm (19). The level of adhesion rapidly rises to a value of near -1 μN after which probe/substrate contact begins, subsequently leading to repulsive loads at about 33 nm. After reversing the sample motion at a peak load of about 20 μN , hysteresis immediately develops and a large adhesive contact is formed reaching levels near -3 μN at about 29 nm. At displacements slightly less than 29 nm, the adhesive contact suddenly ruptures and the interfacial force rapidly returns to zero. The fact that the rupture occurs at a displacement value considerably removed from the original contact suggests that the strong adhesive interaction has caused the Au surface to neck toward the probe as it is withdrawn, narrowing and eventually failing. This galling behavior is very similar to that found in clean-surface modeling of metal probe/metal

substrate interactions (4). Overall behavior similar to that shown in Fig. 2A has been reported earlier for a similarly prepared Au sample (5).

We can better visualize the galling effect of the tip/substrate interaction illustrated in Fig. 2A by using the scanning capability of the IFM to actually image the Au surface. Images of this kind are taken in the constant repulsive-force mode at a force level of 0.2 μN . (Note: this loading value is insufficient to break through the contaminant layer --see Fig. 2B--and permits images to be obtained without galling). The result of this procedure is shown in Fig. 2B which covers a scanning area of 300x300 nm. The height scale in all images has been magnified by 10x to better illustrate the surface topography. The image contrast is such as to give the effect of lighting from left to right. One can see the general morphological structure of the polycrystalline surface, with features having dimensions of a few hundred nanometers, along with several sharp depressions (one of these is marked by an arrow). The depressions are not present in images of the surface prior to loading-cycle measurements. Line scans reveal a height relief of a few tens of nanometers and show that the depressions have widths and depths of several tens of nanometers. The sides of the depressions are very steep supporting the notion that large chunks of Au have been torn from the substrate surface during the necking/rupture process described earlier. In support of this contention, we find that the general resolution of images taken after the loading cycle is enhanced, indicating that the morphological structure of the probe has been altered (sharpened). The original image quality can be regained by subsequently field-desorbing Au from the probe surface, since it has a low desorption field strength (15). The procedure can be repeated with similar results providing compelling evidence for Au transfer.

For a monolayer-covered surface, we can determine the stress level corresponding to the threshold for plastic deformation by taking load-cycle data of the kind shown in Fig. 1 to higher loading levels. Figure 3A shows such data, taken in the

same surface region as was used in Fig. 1A, up to a peak load of 27 μN . In contrast to Fig. 1A, a strong hysteresis is observed over the entire loading cycle. This behavior indicates that plastic or permanent deformation of the Au surface is occurring at these high loading levels. We can estimate the loading threshold for plastic deformation by comparing the loading curve with that predicted by the elastic analysis. Since this is the same surface as probed in Fig. 1, the elastic portion of the loading curve of Fig. 1A can be characterized by the same Hertzian model function used earlier. The comparison is shown in Fig. 3B, where the point-of-contact has been shifted to compensate for the different starting point for the loading cycle. We see that past the region involving film compression, the substrate loading behavior follows the model function only over a limited region increasing less rapidly at the higher loading levels. Thus, the data of Fig. 3B shows that the loading threshold for plastic deformation is above 15 μN , which we determined to represent a maximum shear stress of approximately 1.0 GPa.

It should be noted that the model function, even if shifted, does not describe the unloading portion of Fig. 3A. This is due to the fact that the latter involves the elastic unloading of our parabolic punch embedded in a small socket created by the previous loading deformation. The relationship between load and displacement is quite different in this region. Importantly, it should also be noted that even after the Au sample has been significantly deformed there is still no evidence for tip-substrate adhesive interactions.

We can again verify the deformation of the Au substrate by imaging the surface before and after the high level loading-cycle measurements. These comparisons are shown in Fig. 4A and 4B taken before and after a loading cycle to 57 μN , respectively. The images were processed similarly to that shown in Fig. 2B, except here color-height contrast is used and the images are presented in perspective. The surface

defect in the upper left-hand corner serves as a reference point to evaluate instrumental drift during the 10 min data acquisition period.

The Au-substrate damage caused by the loading cycle of Fig. 2A is confirmed by the second image, Fig. 4B, which clearly shows the presence of an indentation in the middle of the image that was not originally present. The details of the shape of the deformed area are better illustrated by subtracting the first image from the second one, which is shown in Fig. 4C. Treating the data in this manner eliminates the general surface morphological structure, as well as the defect in the upper left hand corner, and confirms the stability of the instrument. In addition, line scans through the center of the deformed area give a quantitative measure of the width and depth of the deformation, which yields values of approximately 51 nm and 2.8 nm, respectively. From these values, assuming a parabolic probe shape, we calculated a tip radius of curvature of 460 nm, in good agreement with the SEM results and our Hertzian deformation analysis.

Conclusions

In agreement with earlier results (5), we have shown that the strong adhesive interaction between a W probe and bare Au substrate results in plastic deformation under negligible applied loads. Probe removal results in galling which transfers Au to the probe surface. In the presence of an adsorbed monolayer of self-assembling docosanethiol molecules ($\text{CH}_3(\text{CH}_2)_{21}\text{SH}$), however, the W/Au interaction is passivated and we observe elastic deformation of the substrate up to shear-stress levels of approximately 1.0 GPa and compressive stress values of 3.4 GPa. Above this stress, the substrate is permanently deformed. However, even in the presence of gross deformation, the film maintains its passivating properties and negligible adhesion is observed upon probe withdrawal. The ability of the monolayer film to

passivate at high loading levels, up to 57 μN (see Fig. 4), is in contrast to the behavior of the contaminant layer on the thiol-free Au surface. Here, metal/metal passivation is only maintained to load levels of about 0.4 μN . At higher loads, the probe displaces the layer and forms a strong adhesive bond galling the surface upon probe withdrawal. The strong monolayer/Au interaction is the key feature differentiating these contrasting behaviors.

It has long been recognized that an adhesive interaction between probe and substrate in indenter experiments can have a dramatic effect on the measured contact deformations (20). The interaction gives rise to an enhanced production of defects in the high-stress region near the edges of the contact area, an effect which is dramatically illustrated by recent model calculations (21). In addition, studies have shown that oxide and carbon contamination films greater than about 50 Å thick on metal surfaces can cause large changes in mechanical behavior (22). However to our knowledge, the present results are the first to show such dramatic alterations in mechanical properties involving the intervention of only a single molecular monolayer, which itself cannot contribute a significant film stiffness.

From a materials standpoint, the shear stress at yield for Au has been predicted to be 0.74 GPa (18). Our results agree within 25% of this prediction suggesting that we are measuring the intrinsic yield behavior of the Au substrate. Since the self-assembling films are incapable of supporting shear stress themselves, these results show that the passivation of the interfacial adhesive force is primarily responsible for our ability to explore the intrinsic surface mechanical behavior. It is clear that films which are stable under high loads can play an important role in surface mechanical-property studies of materials and show great potential for aiding in understanding the role of the interface in defect production and migration.

REFERENCES

1. S. A. Joyce, R. C. Thomas, J. E. Houston, T. A. Michalske, R. M. Crooks, *Phys. Rev. Lett.* **68**, 2790 (1992).
2. J. E. Houston and T. A. Michalske, *Nature* **356**, 266 (1992).
3. G. S. Ferguson, M. K. Chaudhury, G. B. Sigal, G. M. Whitesides, *Science* **253**, 776 (1991).
4. U. Landman, W. D. Luedtke, N. A. Burnham, R. J. Colton, *Science* **248**, 454 (1990).
5. N. A. Burnham and R. J. Colton, *J. Vac. Sci. Technol. A* **7**, 2906 (1989).
6. S. A. Joyce and J. E. Houston, *Rev. Sci. Instrum.* **62**, 710 (1991).
7. R. G. Nuzzo and D. L. Allara, *J. Am. Chem. Soc.* **105**, 4481 (1983).
8. C. D. Bain, E. B. Troughton, Y.-T. Tao, J. Evall, G. M. Whitesides and R. G. Nuzzo, *J. Am. Chem. Soc.* **111**, 321 (1989), and references therein.
9. C. E. D. Chidsey and D. N. Loiacono, *Langmuir* **6**, 682 (1990), and references therein.
10. P. Fenter, P. Eisenberger, Jun Li, N. Camillone, S. Bernasek, G. Scoles, T. A. Ramanarayanan and K. S. Liang, *Langmuir*, **7**, 2013 (1991).
11. M. D. Porter, T. B. Bright, D. L. Allara, C. E. D. Chidsey, *J. Am. Chem. Soc.* **109**, 3559 (1987).
12. R. G. Horn, J. N. Israelachvili and F. Pribac, *J. Coll. Interf. Sci.* **115**, 480 (1987); J. N. Israelachvili and D. Tabor, *Proc. Roy. Soc. Lond.* **A331**, 19 (1972).
13. J. B. Pethica and W. C. Oliver, *Phys. Scr.* **T19**, 61 (1987).
14. K. B. Lodge, *Adv. Coll. Interface Sci.* **19**, 27 (1983).
15. T. T. Tsong, *Atom-Probe Field Ion Microscopy* (Cambridge Univ. Press, New York, 1990), Chap 2.
16. I. N. Sneddon, *Int. J. Engr. Sci.* **3**, 47 (1965).

17. S. P. Timoshenko and J. N. Goodier, *Theory of Elasticity* (McGraw-Hill Book Company, New York, 1970).
18. A. Keliey and N. H. Macmillan, *Strong Solids* (Clarendon Press, Oxford, 1986).
19. This process is described in detailed theoretical modeling for a Ni tip interacting with a Au surface covered by *n*-hexadecane molecules by U. Landman, W. D. Luedtke and E. M. Ringer, *Wear* **153**, 3 (1992).
20. See, for example; K. L. Johnson, K. Kendall and A. D. Roberts, *Proc. Roy. Soc. Lond.* **A324**, 301 (1971); B. V. Derjaguin, V. M. Muller and Yu. P. Toporov, *J. Coll. Interface Sci.* **53**, [2] (1975).
21. U. Landman and W. D. Luedtke, *Science* **248**, 454 (1990).
22. D. Pashley, J. B. Pethica, D. Tabor, *Wear* **100**, 7 (1984); N. Gane, *Proc. Roy. Soc. Lond.* **A317**, 367 (1970).
23. The authors wish to thank S. A. Joyce for his many helpful discussions. R.C.T. acknowledges the support of Associated Western Universities through a DOE Laboratory Graduate Fellowship. J.E.H. and T.A.M. acknowledge support by the Office of Basic Energy Sciences, Division of Material Sciences, U.S. Department of Energy under Contract No. DE-AC04-76DP00789. R.M.C. acknowledges the support of the Office of Naval Research (Young Investigator Program).

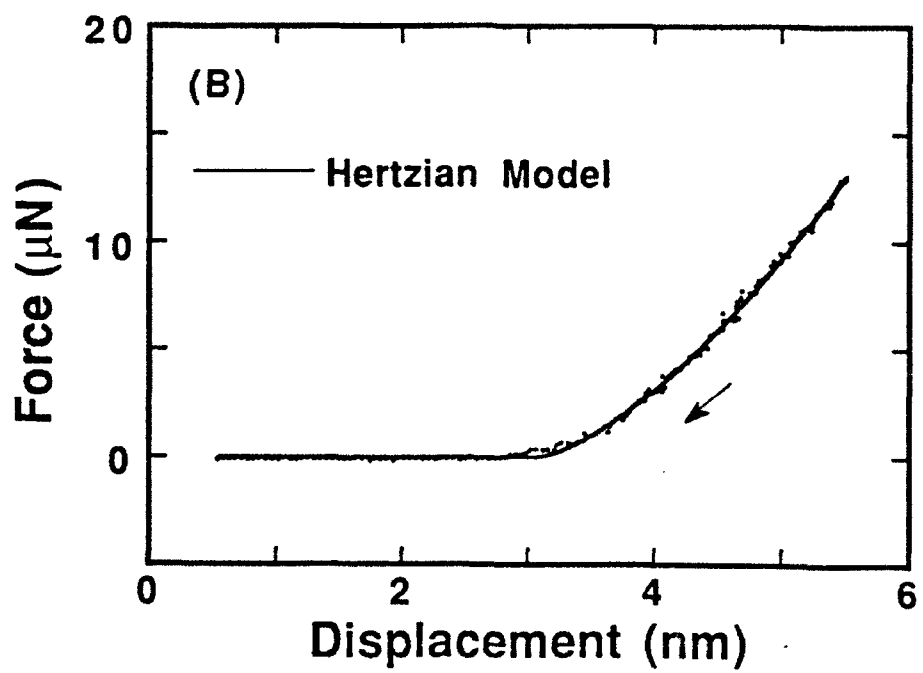
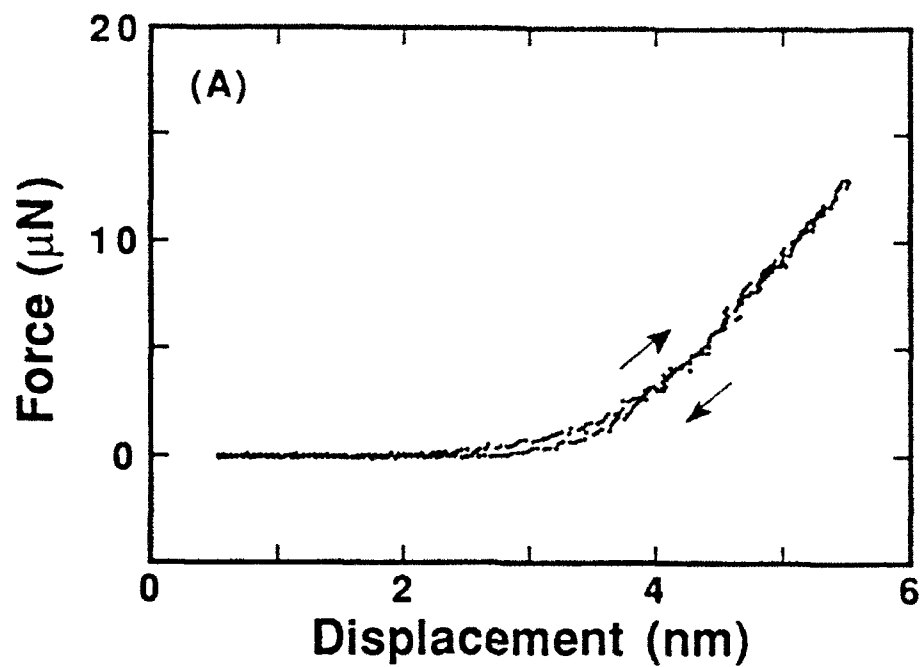
FIGURE CAPTIONS

Fig. 1. (A) Interfacial force vs. displacement (loading cycle) behavior for a Au surface covered with a $\text{CH}_3(\text{CH}_2)_{21}\text{SH}$ monolayer film interacting with W probe having a parabolic shape with a radius of curvature at its apex of approximately 500 nm. Zero displacement represents an arbitrary starting and ending position and positive values indicate repulsive forces. (B) Withdrawal curve of the loading cycle in (A) compared with the Hertzian model function (16) for a rigid parabolic punch indenting an elastic half space (the solid line).

Fig. 2. (A) Loading cycle for a Au substrate, in the absence of a methyl-terminated monolayer film, interacting with the W probe used to obtain the data shown in Fig. 1. (B) Repulsive-force images of the Au surface after the loading cycle of (A) taken at a constant repulsive load of $0.2\ \mu\text{N}$. The relative height scale has been magnified by 10x.

Fig. 3. (A) Loading-cycle measurement for a monolayer covered Au substrate up to repulsive load of approximately $27\ \mu\text{N}$. The W probe is the same as that used in Fig. 1. (B) Data obtained from (A) plotted against the Hertzian model function obtained in Fig. 1B. The point-of-contact for this function has been shifted to account for the change in the loading-cycle starting point.

Fig. 4. Constant repulsive-force images of Au covered by a $\text{CH}_3(\text{CH}_2)_{21}\text{SH}$ monolayer film. (A) Image before any permanent damage occurred to the Au surface. (B) Image taken immediately after a force profile to a peak load of $57\ \mu\text{N}$. (C) A difference image resulting from the subtracting of (B) from (A). The relative height scales have been magnified by 10x.



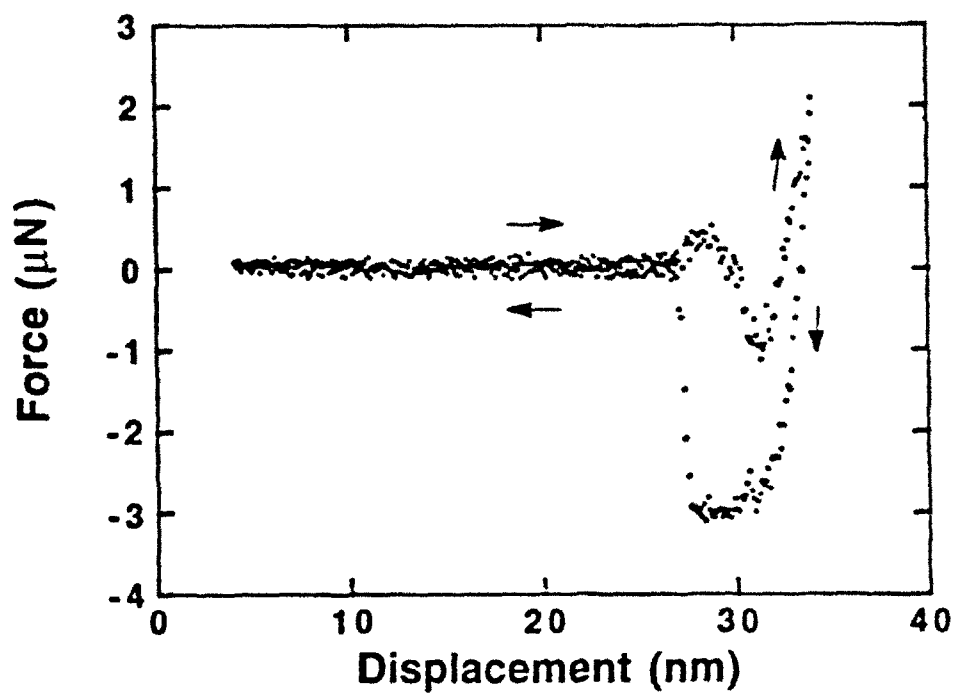
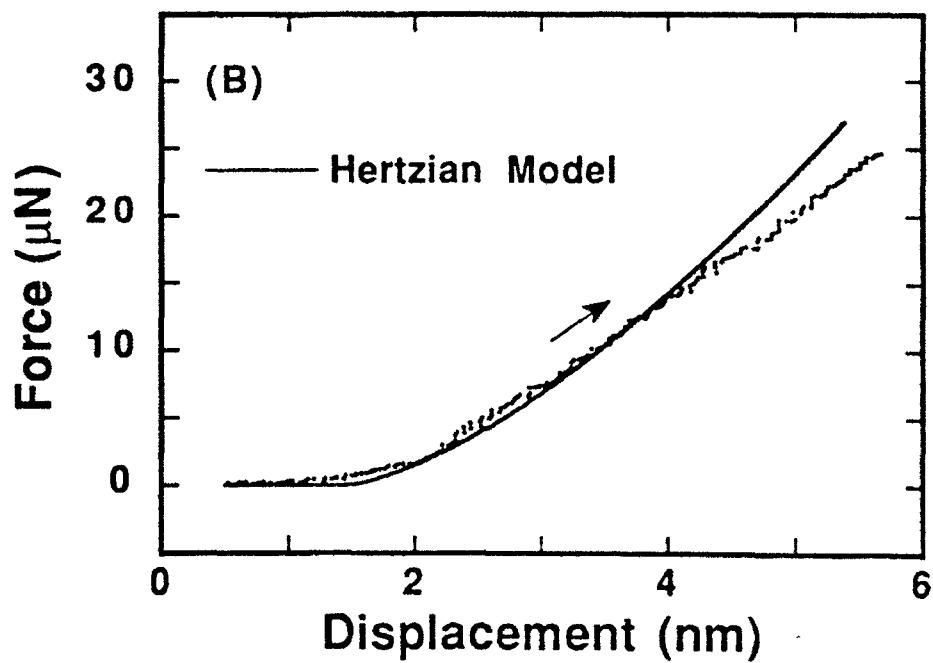
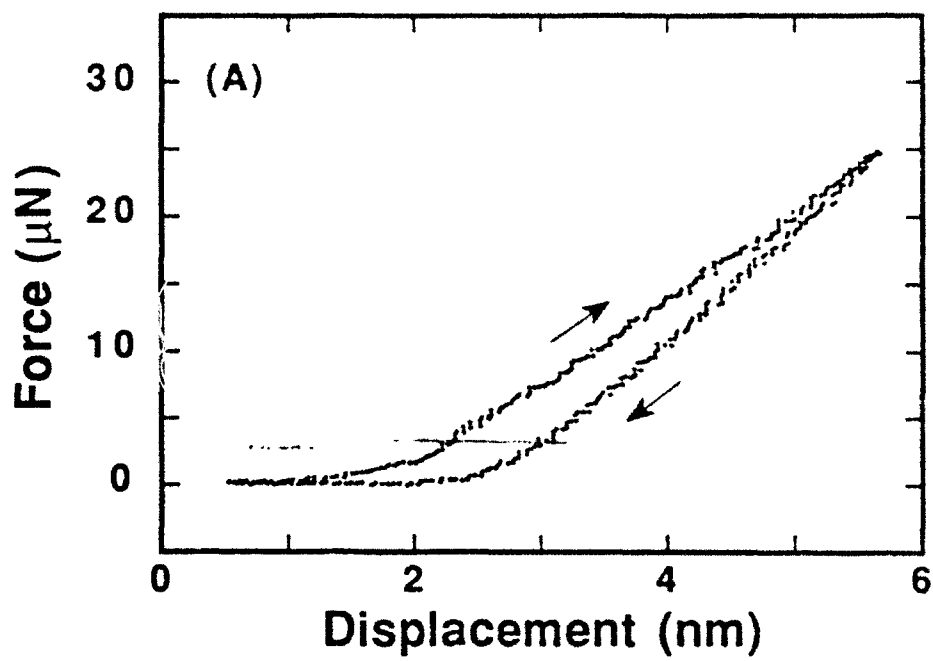


Fig. 2



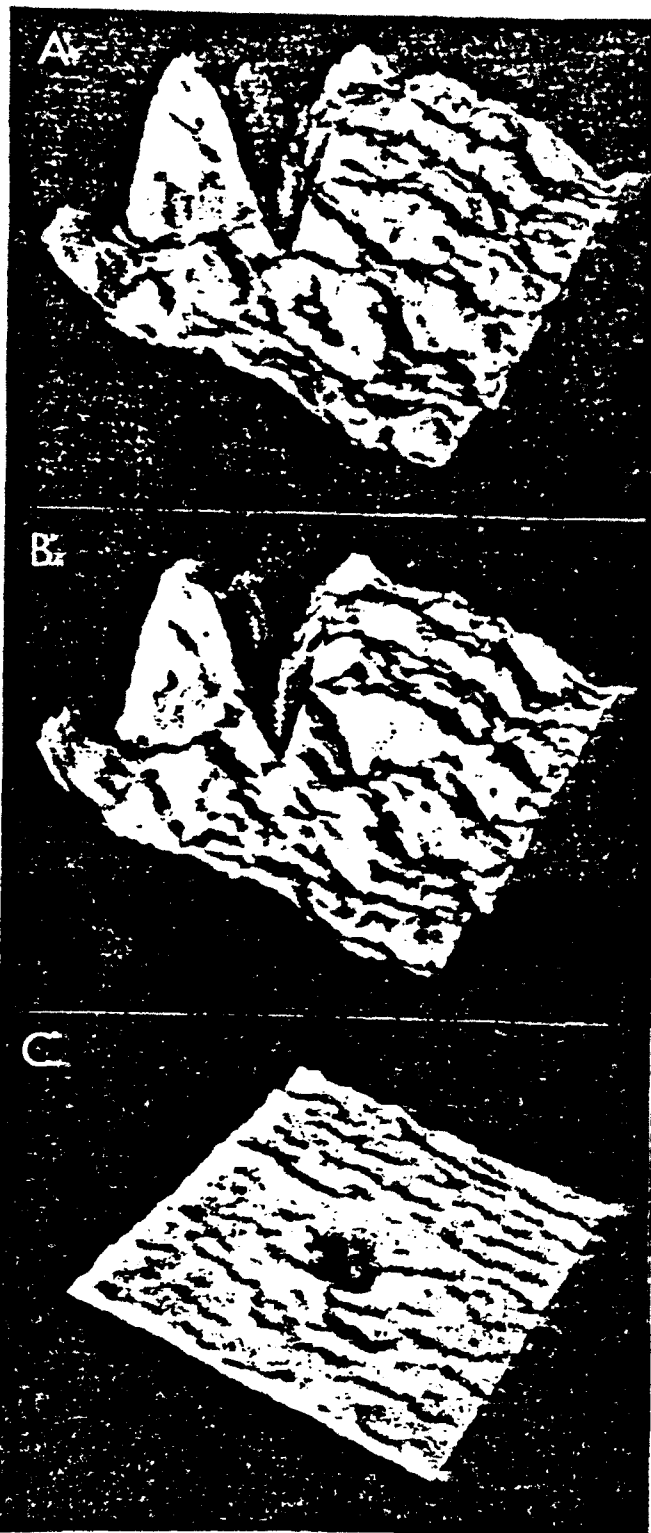


Fig. 4

TECHNICAL REPORT DISTRIBUTION LIST - GENERAL

Office of Naval Research (2)*
Chemistry Division, Code 1113
800 North Quincy Street
Arlington, Virginia 22217-5000

Dr. Richard W. Drisko (1)
Naval Civil Engineering
Laboratory
Code L52
Port Hueneme, CA 93043

Dr. James S. Murday (1)
Chemistry Division, Code 6100
Naval Research Laboratory
Washington, D.C. 20375-5000

Dr. Harold H. Singerman (1)
Naval Surface Warfare Center
Carderock Division Detachment
Annapolis, MD 21402-1198

Dr. Robert Green, Director (1)
Chemistry Division, Code 385
Naval Air Weapons Center
Weapons Division
China Lake, CA 93555-6001

Dr. Eugene C. Fischer (1)
Code 2840
Naval Surface Warfare Center
Carderock Division Detachment
Annapolis, MD 21402-1198

Dr. Elek Lindner (1)
Naval Command, Control and Ocean
Surveillance Center
RDT&E Division
San Diego, CA 92152-5000

Defense Technical Information
Center (2)
Building 5, Cameron Station
Alexandria, VA 22314

Dr. Bernard E. Douma (1)
Crane Division
Naval Surface Warfare Center
Crane, Indiana 47522-5000

* Number of copies to forward